Particle Motions in a Gas-Fluidized Bed of Sand

Narayanan Menon and Douglas J. Durian
Department of Physics and Astronomy, University of California, Los Angeles, California 90095-1547
(Received 27 May 1997)

We report measurements by diffusing-wave spectroscopy of particle motions in a gas-fluidized bed. The homogenous state of the bed known as the uniformly fluidized state is actually a weak *solid* in which particles are at rest. The only truly fluid state is an inhomogenous mixture of gas bubbles and of liquid regions in which microscopic particle dynamics are shown to be collisional. The motion of macroscopic bubbles is the source of particle motions in the bed. Measurements of mean free paths, collision rates, and velocity fluctuations (the "granular temperature") show that dissipation occurs nonuniformly in the medium. [S0031-9007(97)04395-0]

PACS numbers: 46.10.+z, 47.55.Kf, 47.55.Mh

A gas-fluidized bed [1] is a system of randomly arranged, macroscopic grains in which motions are excited by an interstitial flow of gas. This system is of tremendous technological importance [1] in catalysis of gas-phase reactions, transport of powders, combustion of ores, and several other industrial processes. More fundamentally, it is an ideal venue in which to study the transition of a granular system [2] from a solidlike to a liquidlike phase under the influence of external forces. Gas fluidization is complementary to other means of fluidization such as vibration [3] and shear [4], where the system is driven inhomogenously by impact or friction at the boundaries. An important step towards a hydrodynamic description of any granular "fluid" is to trace the flow of the dynamics from long length scales, where external forces drive mechanical energy into the system, down to the microscopic level, where energy is lost via collisions between grains. Several theoretical efforts [5] towards building such a granular fluid mechanics start by considering the medium as a dense, inelastic gas with a temperature defined by local velocity fluctuations. Experimental efforts to probe this picture have been frustrated by two problems. First, strong scattering of visible light at the surfaces of grains makes granular systems inherently opaque to conventional optical techniques. Second, while the particles themselves are macroscopic, the temporal and spatial scales at which collisions occur can be much smaller than optical or magnetic resonance imaging is able to resolve.

In this Letter, we report results from diffusing-wave spectroscopy (DWS) [6] measurements where we take advantage of the multiple light scattering from grains to interrogate their relative motions. DWS is noninvasive and is sensitive to very short length (10^{-8} to 10^{-4} cm) and time scales (10^{-8} to 1 s), allowing us to precisely characterize particle dynamics in the interior of the system. We demonstrate that the medium is liquefied only when driven hard enough that macroscopic bubbles rise through the system. The medium is then in a spatially inhomogenous state in which gas bubbles and liquid (and perhaps solid) regions coexist. We quantify dynamics in the liquid in terms of collision rates, mean free paths, and the so-called "granular temperature" and find that dissipation occurs nonuniformly even within the liquid phase. As the external driving force is decreased to just above the point where the grains are neutrally buoyant, the system is in a homogenous state known as the uniformly fluidized state. We show that the uniform fluid is not a fluid at all, but rather a weak, and absolutely static, solid.

The granular medium in our fluidized bed is made up of spherical glass beads (Cataphote Inc.) of diameter 49 ± 4, 96 ± 10, or 194 ± 17 μm. The beads are contained in a glass tube of square cross section ($A = 6$ cm $\times$ 6 cm) and are supported from below by a porous glass frit, which also serves as a gas diffuser. Dry N_2 is introduced at fixed base pressure through a wind box below the frit. We use DWS to probe any accompanying microscopic particle motions. For this, the sample is illuminated by an Ar^+ laser with $\lambda = 514$ nm and beam diameter $\approx$3 mm. Incident photons are scattered by the beads and execute random walks in the sample. Some of these diffusive walks reemerge on the incident face of the sample and interfere to produce a speckle pattern which we sample through a 50 μm pinhole with a photomultiplier tube connected to a correlator. The autocorrelation function of the intensity fluctuations of the speckles in this backscattering geometry [7] is then interpreted [6] in terms of the dynamics of the beads.

Figure 1 describes two macroscopic probes of the response of the bed as the gas flow rate is increased from zero. In Fig. 1(A), we show $(h - h_0)/h_0$, the fractional change in height of the bed as a function of the superficial gas velocity, U_s ($\equiv$ volume flow rate/A). In Fig. 1(B), we show $\Delta P/\rho g h$, the pressure drop experienced by the gas across the bed normalized by the weight of the entire bed per unit area. Three distinct regimes of behavior are observed as U_s is increased from zero. The first of these is at small values of U_s where the bed height remains constant [Fig. 1(A)]. In this regime the pressure drop, ΔP, varies linearly with U_s [Fig. 1(B)] and with depth, as expected from Darcy's law. The bed shows all the properties of a static heap of sand such as a finite angle of repose at its surface. Since this is a static ensemble of scatterers, no motions are detected by DWS.

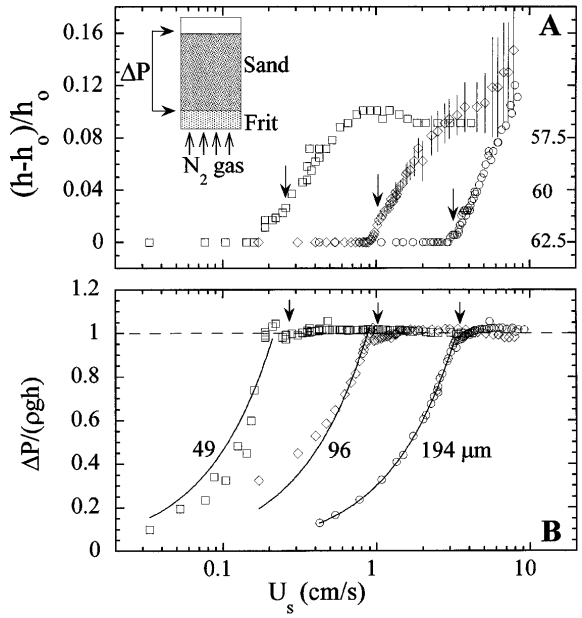

FIG. 1. Macroscopic probes of fluidized beds with particles of diameter $D = 49$, 96, or 194 μm ($\square$, $\diamond$, $\bigcirc$, respectively). (A) The fractional change in height (h) of the bed relative to its height at zero gas flow ($h_0 \approx 15$ cm) vs superficial gas velocity, U_s in cm/s. The bars show typical fluctuations of the height of the bubbling bed. On the right axis are equivalent packing percentages (the random loose and close packing limits are 56% and 63.5%). (B) The gas pressure drop across the bed, ΔP, normalized by $\rho g h$ (where ρ is the average density). The curves are linear fits in the unfluidized regime. The arrows indicate the onset of bubbling.

The second regime occurs above a well-defined value of U_s called the minimum fluidization velocity, U_{MF}, when ΔP becomes equal to the weight of the bed [i.e., the normalized pressure in Fig. 1(B) equals 1] and the bed expands homogeneously. In this state, the medium behaves qualitatively like a fluid: the angle of repose drops to zero and dense objects sink while light ones float. This is said to be the "uniformly fluidized state" [8]. Surprisingly enough, no intensity fluctuations are seen in the uniformly fluidized state. Since DWS is sensitive to motions down to 1 Å, this implies that *the uniformly fluidized state is a completely static state.* It has long been a matter of debate as to whether stresses in this state are carried by particle contacts or by collisions. Careful measurements of stable density inhomogeneities and hysteresis as a function of U_s led Tsinontides and Jackson [9] to suggest that some contact stresses must persist in the uniform fluid. Our measurements directly show that essentially *all* particles in the system are held by enduring contacts. The seemingly fluidlike response is due to the fact that frictional forces (which scale with the normal forces that beads exert on each other) have become exceedingly small.

The third regime occurs when U_s is increased beyond a threshold gas velocity [see arrows in Figs. 1(A) and 1(B)], where gas flow through the system becomes inhomogenous, with some gas rising up as bubbles that have a well-defined interface with the surrounding granular medium and a characteristic mushroom-cap shape. In this regime, the bed continues to expand as U_s is increased, with no further change in ΔP. The first motions detected by DWS coincide with the visual observation of the onset of bubbling. Therefore, *bubble motion is the source of all particle dynamics in the bed.* As bubbles rise, they induce bulk downward flows of grains on which are superimposed microscopic random motions. The relative mean square displacement $\langle \Delta r^2(\tau) \rangle$ of 96 μm beads is plotted in Fig. 2 for several values of U_s. At short times, we find $\langle \Delta r^2(\tau) \rangle \propto \tau^2$, which indicates ballistic motion of beads relative to each other with a randomly directed velocity, $\delta V^2 = \langle \Delta r^2(\tau) \rangle / \tau^2$. The ballistic motion terminates at a time τ_c, characteristic of collisions between beads. At times $\tau > \tau_c$, the relative positions of particles change only very slowly as reflected in the slow increase in $\langle \Delta r^2(\tau) \rangle$ with τ. The crossover from ballistic motion to the long-time behavior is similar to that observed [10] in a gravity-driven, granular flow where the long-time limit is found to be diffusion superimposed on the convective flow. This extended subdiffusive crossover is attributed to motion of a particle "caged" by its neighbors and has parallels in thermal systems such as correlated liquids and dense colloids.

As U_s is increased, bulk flows speed up and so do the accompanying microscopic motions, as may be seen in the shift of the curves of Fig. 2 to shorter time. In Figs. 3(A) and 3(B) we show that as U_s is increased beyond the onset of bubbling the collision time τ_c decreases and the velocity fluctuation δV increases rapidly, but both settle down to a slower rate of change at large values of U_s/U_{MF}. We currently do not know what sets the

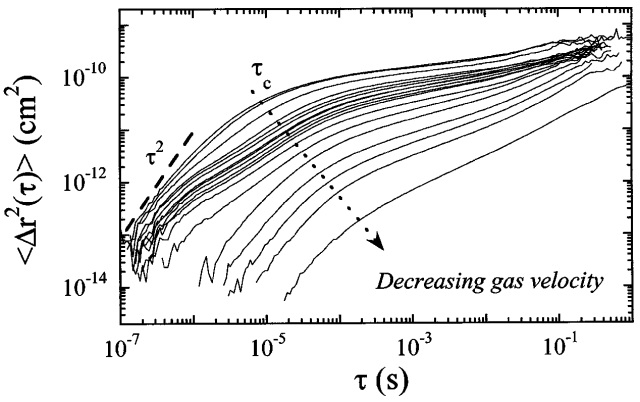

FIG. 2. DWS results for mean square displacement of beads, $\langle \Delta r^2(\tau) \rangle$ (in cm^2), as a function of time, τ (in sec) in a bed of 96 μm beads. The short time dynamics are collisional with $\langle \Delta r^2(\tau) \rangle = \delta V^2 \tau^2$ for $\tau < \tau_c$, the collision time. As U_s is increased, the collisional regime shifts to shorter times and higher velocities. For $\tau > \tau_c$, $\langle \Delta r^2(\tau) \rangle$ changes very slowly with τ for several decades in time.

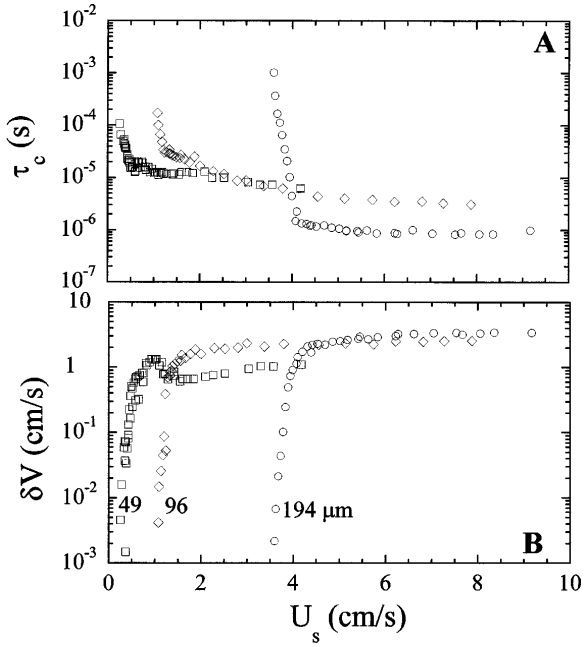

FIG. 3. Dependence on gas velocity, U_s, of parameters of the collisional regime: (A) Velocity fluctuations, δV, and (B) collision time, τ_c. Both sets of parameters change rapidly beyond the onset of bubbling [12] and thereafter turn over to a slower variation with U_s. (□, ◇, ○ are $D = 49$, 96, or 194 μm, respectively).

scale for either of these quantities in terms of the gas flow rate and material parameters. Since δV, the magnitude of velocity fluctuations, is used in place of temperature in kinetic theories of granular media [5], it is a crucial experimental input in evaluating any such formulation. The measurements of Ref. [10] are the only experimental determination of δV in the interior of a 3D granular system. However, δV has been extracted at the surface of a gas-fluidized bed by Cody *et al.* [11] using the acoustic response of the container to particle collisions. Our results are in qualitative agreement with theirs, showing that the "temperature" of the particles colliding with the wall shows the same trends as those determined by DWS, which averages over several bead diameters.

How does the gas flow drive these microscopic motions? At a macroscopic level the distribution of gas between bubbles and the bulk, and the balance of pressures and energy between gas flow and grains has often been described within the two-fluid model [1]. In the simplest version, the dense granular phase has constant density and is uniformly heated by a bubble phase which provides a path for all gas in excess of minimum fluidization, $(U_s - U_{\mathrm{MF}})$, with no additional pressure drop. This qualitatively explains the fact that ΔP does not increase beyond U_{MF}. Furthermore, this implies that the volume flux of excess gas entering the bed equals the volume flux of bubbles through any cross section,

$$A(U_s - U_{\mathrm{MF}}) = AV_b(h - h_0)/h_0\,, \qquad (1)$$

where V_b is the average bubble velocity. The volume fraction occupied by bubbles is estimated by $(h - h_0)/h_0$, the fractional expansion of the bed shown in Fig. 1(A). In Fig. 4(A) we show that the value of V_b computed from Eq. (1) agrees fairly well with that obtained from video imaging of bubbles near the walls of the bed, thus supporting the two-fluid assumption regarding gas volume in the bubbles.

The two-fluid picture thus gives a reasonable budget of pressure and gas volume. Additionally, as follows, it shows that the energy used in forcing gas through the bed in excess of U_{MF} is expended mainly in bubble motion. The power dissipated in transporting a bubble of volume Ω is given by $\Omega\rho g V_b$. Using Eq. (1) and $\Delta P = \rho g h$, the dissipation rate per volume in the bed equals

$$\left(\frac{h - h_0}{h_0}\right)\rho g V_b = \left(\frac{U_s - U_{\mathrm{MF}}}{V_b}\right)\rho g V_b = (U_s - U_{\mathrm{MF}})\,\frac{\Delta P}{h}\,, \qquad (2)$$

which exactly equals the excess power input.

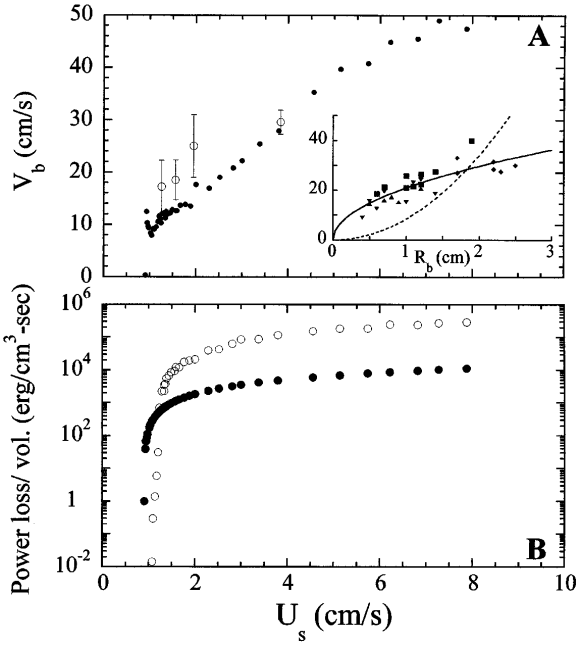

FIG. 4. (A) Dependence of bubble velocity, V_b (cm/s), on superficial gas velocity, U_s, in the 96 μm beads. A simple two-fluid prediction (●), $V_b = (U_s - U_{\mathrm{MF}})h_0/(h - h_0)$ compares well with direct measurements by video microscopy (○). The bars on the latter reflect a distribution of velocities due to a spread in bubble size, R_b. The dependence of V_b on R_b (in cm) is shown in the inset. The solid line represents the function $0.67(gR_b)^{1/2}$, and the dashed line is a fit to an R_b^2 dependence, corresponding to a balance between Stokes drag and gravity. (B) The power expended per volume on the gas in excess of that required for minimum fluidization (●), $\Delta P(U_s - U_{\mathrm{MF}})$, is greater than the rate of energy dissipated per volume in collisions (○), $(1/2)(1 - e^2)\rho(\delta V)^2/\tau_c$ (where coefficient of restitution, $e = 0.9$).

This work drives flows in the bed and ultimately leaves the system due to inelastic collisions. We can estimate collisional losses from the parameters obtained by DWS. In Fig. 4(B) we show that these inelastic losses (from regions probed by DWS near the walls) are far in excess of the gas losses (averaged over the whole bed). This difference can be reconciled if dissipation is inhomogenous across the bed, a reasonable possibility given that dissipation is intimately associated with bubble motion. It is also reasonable since bubble motion produces inhomogenous particle flows. In the bubbling state, tracer beads are carried in large-scale convection patterns with a downflow at the walls and an upflow in the middle of the bed. Superimposed on this overall convection are motions in the vicinity of a rising bubble, where particles are swept up with the bubble. The data of Fig. 3 therefore represent the evolution of the time-averaged dynamics in the downflow at the walls rather than an average over the entire bed.

In conclusion, we have shown directly that there are no particle motions in the uniformly fluidized state of the bed. This state is, in fact, a weak solid rather than a fluid despite the fact that the system is not held together by gravity. The viscous drag of the gas is uniform on all the particles in the solid, and one might have expected it to melt into a homogenous liquid phase. However, fluidity is initiated by the instability to bubbling, and therefore the liquid phase is always inhomogenous. The stability of bubbles is itself an interesting issue in a hard-sphere system with no cohesive forces and presumably no surface tension. Since bubbles drive dynamics in the bed, a better experimental understanding of the flow field of particles created by a single bubble would also be crucial to understanding the complex, inhomogenous convection of particles in the bubbling bed.

We thank G. D. Cody, R. Bruinsma, A. J. Liu, and R. Jackson for useful conversations. We are grateful to NASA and NSF for financial support.

[1] *Fluidization,* edited by J. F. Davidson, R. Clift, and D. Harrison (Academic, London, 1985); *Gas Fluidization Technology,* edited by D. Geldart (Wiley-Interscience, New York, 1986).

[2] H. M. Jaeger, S. R. Nagel, and R. P. Behringer, Rev. Mod. Phys. **68**, 1259 (1996); C. S. Campbell, Annu. Rev. Fluid Mech. **22**, 57 (1990).

[3] E. Clement and J. Rajchenbach, Europhys. Lett. **16**, 133 (1991); J. B. Knight *et al.,* Phys. Rev. E **54**, 5726 (1996); S. Warr, J. M. Huntley, and G. T. H. Jacques, *ibid.* **52**, 5583 (1995); A. Kudrolli, M. Wolpert, and J. P. Gollub, Phys. Rev. Lett. **78**, 1383 (1997).

[4] O. Zik *et al.,* Phys. Rev. Lett. **70**, 2431 (1994); D. M. Hanes and D. L. Inman, J. Fluid Mech. **150**, 357 (1985).

[5] R. A. Bagnold, Proc. R. Soc. London A **225**, 49 (1954); J. T. Jenkins and S. B. Savage, J. Fluid Mech. **130**, 187 (1983); P. K. Haff, *ibid.* **134**, 401 (1983).

[6] G. Maret and P. E. Wolf, Z. Phys. B **65**, 409 (1987); D. J. Pine *et al.,* Phys. Rev. Lett. **60**, 1134 (1988); D. A. Weitz and D. J. Pine, in *Dynamic Light Scattering,* edited by Wyn Brown (Clarendon, Oxford, 1993), pp. 652–720.

[7] Intensity fluctuations in transmission result not only from particle dynamics but also from changes in optical thickness as bubbles pass between the light source and detector. In backscattering, however, the medium is always effectively semi-infinite.

[8] This regime is not observed for $D = 194$ μm beads, which go directly into the third regime above $U_s = U_{\mathrm{MF}}$. Apart from D, the range of uniform fluidization depends on geometry and boundary conditions.

[9] S. C. Tsinontides and R. Jackson, J. Fluid Mech. **255**, 237 (1993).

[10] N. Menon and D. J. Durian, Science **275**, 1920 (1997).

[11] G. D. Cody *et al.,* Powder Technol. **87**, 211 (1996).

[12] The nonmonotonic variation of δV with U_s in the 49 μm beads versus the monotonic increase seen in larger beads has been emphasized in Ref. [11] as a trend in a microscopic quantity that correlates with the tendency to show uniform fluidization before bubbling.